

*Original Research*

# Synthesis of Novel Core-Shell Magnetic Fe<sub>3</sub>O<sub>4</sub>@C Nanoparticles with Carboxyl Function for Use as an Immobilisation Agent to Remediate Lead-Contaminated Soils

Chuang Ma<sup>1</sup>, Fu-Yong Liu<sup>1</sup>, Ming-Bao Wei<sup>1,2</sup>, Ji-Hong Zhao<sup>2</sup>, Hong-Zhong Zhang<sup>2\*</sup>

<sup>1</sup>School of Materials and Chemical Engineering, Zhengzhou University of Light Industry, Zhengzhou, China

<sup>2</sup>Henan Collaborative Innovation Center of Environmental Pollution Control and Ecological Restoration, Zhengzhou University of Light Industry, Zhengzhou, China

*Received: 19 May 2019*

*Accepted: 24 July 2019*

## Abstract

In this study, a carbon shell was coated on Fe<sub>3</sub>O<sub>4</sub> nanoparticles using a hydrothermal method followed by modification of carboxyl end groups on the Fe<sub>3</sub>O<sub>4</sub>@C to form Fe<sub>3</sub>O<sub>4</sub>@C-COOH for creating an immobilisation agent for remediating lead-contaminated soils. The surface of an Fe<sub>3</sub>O<sub>4</sub>@C nanoparticle was successfully covered with carboxyl end groups. The Fe<sub>3</sub>O<sub>4</sub> core possessed the superparamagnetism property; the carbon shell protected the core from being oxidised or dissolved in acid solution, and provided good modifiability. Due to the strong interaction between lead and carboxyl end groups, this synthesised remediation agent exhibited high adsorption capacity. The Fe<sub>3</sub>O<sub>4</sub>@C-COOH nanoparticles principally promoted the transformation of lead (Pb) from a reducible to residual state, while having no obvious effect on the oxidation state of the lead. The amount of Fe<sub>3</sub>O<sub>4</sub>@C-COOH and the composition of soil organic matter had a higher influence on Pb distribution than soil pH, water content, or conductivity. Under optimal immobilisation conditions, the fractionation of the Pb acid-soluble, reducible, oxidative, and residual states in the contaminated soil changed significantly. The leaching and migration of Pb were significantly reduced, thus achieving remediation of lead-contaminated soils by immobilisation. Thus, remediation of lead-contaminated soils via Fe<sub>3</sub>O<sub>4</sub>@C-COOH immobilisation is a potentially practical and technologically feasible method.

**Keywords:** soil, Pb, Fe<sub>3</sub>O<sub>4</sub>@C-COOH, chemical state, immobilisation

## Introduction

In recent decades, contamination of farmland with toxic metals, e.g. lead (Pb) and zinc (Zn), has had an adverse effect on human health through the consumption of food degraded in both quantity and quality [1-2]. Heavy metals cannot be biodegraded [3]; these metals enter the human body through the food chain, where they are accumulated in crops grown in contaminated soils [4-6]. Therefore, it is necessary to immobilise or fully remove heavy metals from agricultural soils in order to provide a safer environment and food sources for humans [7-9]. In order to immobilise or eliminate heavy metals from polluted soils, various methods have been developed, including soil washing, phytoremediation, thermal treatment and electrochemical treatment [3-4] [10]. Among these different techniques, immobilisation of heavy metals using soil amendments has received greater attention as a promising solution for soil remediation [11]. Immobilisation agents are the key factor in determining the success of remediation of heavy metal-polluted soils through immobilisation [7]. Immobilisation of heavy metals in soils by organic matter, phosphate rock, lime, biochar and other traditional remediation agents have been previously studied [12-14]. However, these agents have limitations, such as the lack of specific functional groups leading to poor specificity, high application usage resulting in high costs [7], and the need for a long remediation time [15]. Hence, environmental researchers have been engaged in finding easy, effective, economical, and eco-friendly techniques for the solidification, or immobilisation, of lead ions in soil [16-17].

Recently, the application of nanomaterials in environmental remediation and pollutant removal has become a focus due to certain exceptional properties, such as high surface area, increased absorption, and special photoelectric properties [18]. Magnetic nanomaterials show great potential for removal of heavy metals from water [19-23]. For example, iron oxide nanoparticles have been synthesised in order to remove arsenic (As) and Pb from an aqueous solution [24]. Surface-functionalised magnetic nanoparticles have also been developed for removal and extraction of heavy metals from solution [10, 24]. Although these magnetic nanomaterials have been utilised extensively in wastewater treatment, it should be pointed out that there are few studies on core-shell  $\text{Fe}_3\text{O}_4@\text{C}$  nanoparticles, which have not been reviewed for use in lead-contaminated soil up to now. It follows that there is a high demand to develop novel magnetic nanomaterial remediation agents with high efficiency

and good stability that are also safe in the environment for immobilisation of lead in contaminated soil.

Measurement of total concentrations of heavy metals do not suffice as an assessment of potential risks [1]; chemical fractionation has been used extensively to assess the mobility and bioavailability of heavy metals in soils [4]. Remediation of heavy metal-contaminated soils through immobilisation results in a change in the chemical fraction, or state, of the heavy metal from bioavailable to stable, i.e. inert [15, 25], signalling a significant decrease in biological uptake of heavy metals [4]. In this study, a novel remediation agent of COOH-functionalised carbon-coated  $\text{Fe}_3\text{O}_4$  core-shell nanoparticles ( $\text{Fe}_3\text{O}_4@\text{C-COOH}$ ) was prepared for immobilisation of lead in contaminated soil. We characterised the  $\text{Fe}_3\text{O}_4@\text{C-COOH}$  and investigated the effect of application amount, soil pH, water content, conductivity and organic matter on the distribution of the Pb fraction in soils. Furthermore, the effectiveness of immobilisation of Pb in contaminated soil with the application of  $\text{Fe}_3\text{O}_4@\text{C-COOH}$  nanoparticles is discussed.

## Material and Methods

### Lead-Contaminated Soil

Lead-contaminated soils were collected from the top 25 cm of topsoil from farmland located near a lead-zinc smelter (Longitude 112°33'21"E, Latitude 35°8'26"N) in Ji Yuan, Henan Province, China. The soil Pb concentration was  $737.34 \pm 13.39 \text{ mg}\cdot\text{kg}^{-1}$ , which is 2.46 times higher than the China Soil Environmental Quality Standard ( $300 \text{ mg}\cdot\text{kg}^{-1}$ ). The results of the speciation analysis showed that the proportion of Pb species generally declined in the following order: reducible state (62.04%) > oxidisable state (16.15%) > acid-soluble state (14.69%) > residual state (7.53%).

The soils were naturally air-dried, ground in an agate mortar, sieved through a 100-mesh sieve and packed in bags. The physical and chemical properties of the soil are shown in Table 1.

### Preparation of $\text{Fe}_3\text{O}_4@\text{C-COOH}$

As shown in Fig. 1, monodisperse silicon dioxide ( $\text{SiO}_2$ ) template microspheres with an average diameter of 400 nm were prepared by a modified Stober method and stored after freeze-drying [26].  $\text{SiO}_2@\text{Fe}_3\text{O}_4@\text{C}$  magnetic nanomaterials were prepared as previously described by Cheng [27].  $\text{SiO}_2@\text{Fe}_3\text{O}_4@\text{C}$  was etched

Table 1. Soil physicochemical parameters and distribution of Pb state.

pH	Electrical conductivity ( $\mu\text{s}\cdot\text{cm}^{-1}$ )	Organic matter ( $\text{g}\cdot\text{kg}^{-1}$ )	Total Pb concentration ( $\text{mg}\cdot\text{kg}^{-1}$ )	Acid-soluble state ( $\text{mg}\cdot\text{kg}^{-1}$ )	Reducible state ( $\text{mg}\cdot\text{kg}^{-1}$ )	Oxidisable state ( $\text{mg}\cdot\text{kg}^{-1}$ )	Residual state ( $\text{mg}\cdot\text{kg}^{-1}$ )
7.33±0.02	142.60±2.13	20.13±1.05	737.34±13.39	109.63±3.21	462.99±5.25	120.52±3.34	56.19±2.67

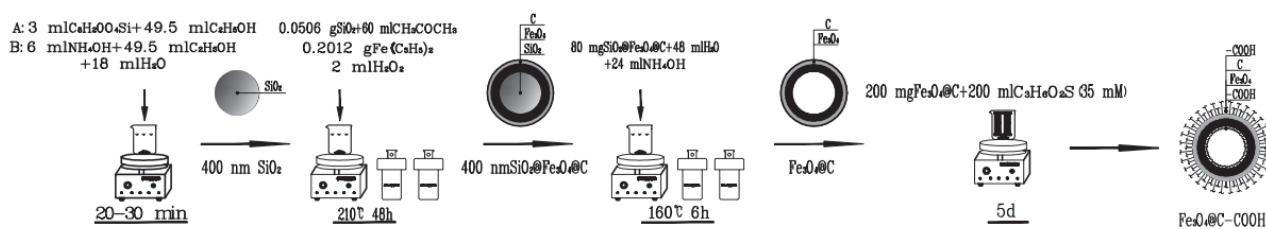


Fig. 1.  $\text{Fe}_3\text{O}_4@\text{C-COOH}$  preparation process.

to form hollow microspheres of  $\text{Fe}_3\text{O}_4@\text{C}$  [27].  $\text{Fe}_3\text{O}_4@\text{C}$  (200 mg) was added to a 200 mL solution of 3-mercaptopropionic acid (35 mM). A colloidal solution of  $\text{Fe}_3\text{O}_4@\text{C-COOH}$  was obtained by ultrasonic dispersion for 1 hour at 400 Watts. Following five days of dialysis (analytical quantity analytical quantity MwCO: 2000D), the hollow  $\text{Fe}_3\text{O}_4@\text{C-COOH}$  nanoparticles were obtained by changing water every half day.

### Material Characterisation Methods

The samples were characterised using X-ray diffraction (XRD) (D8 Advance, Bruker, Germany), and transmission electron microscopy (TEM) (JEM-2100, JEOL Ltd, Japan). The appearance and morphology of the material were characterised by JSM-6490LV (JEOL Ltd, Japan) scanning electron microscopy (SEM). The material was further analysed using a Nicolet iS50 (Thermo Fisher Scientific Inc, US) Fourier transform infrared spectrometer (FT-IR). Magnetic properties of the materials were measured with a vibrating sample magnetometer (VSM) (MPMS3, Quantum Design Inc, US).

### Adsorption Experiments in Water

A series of  $\text{Pb}^{2+}$  solutions with concentrations ranging  $15.0 \text{ mg}\cdot\text{L}^{-1}$  were prepared with  $\text{Pb}(\text{NO}_3)_2$ . Then, 25 mL of the above-mentioned  $\text{Pb}^{2+}$  solution ( $15 \text{ mg}\cdot\text{L}^{-1}$ ) was added to a 40 mL centrifugal tube, and pH of the solutions was adjusted to 6.0. After homogeneous mixing, it was shaken 0, 20, 40, 60, 80, 100, and 120 min respectively by a constant temperature oscillator ( $30^\circ\text{C}$ ) in order to study the effect of adsorption time on the adsorption capacity. At the same time, the pH of the solutions was adjusted within a range of 1.0 to 7.0 using dilute HCl and NaOH in order to study the effect of pH on the adsorption capacity. As a final step, after magnetic separation, the supernatant was evaluated with an atomic absorption spectrometer (ZEEnit-700P, Analytik Jena AG, Jena, Germany).

### Batch Pb Speciation Distribution Experiments in Soil

The Pb speciation distribution experiments were prepared to investigate the effect of  $\text{Fe}_3\text{O}_4@\text{C-COOH}$  application amount, soil pH, water content, conductivity

and organic matter content on soil remediation as follows:

- (1) Application amount (AA) of  $\text{Fe}_3\text{O}_4@\text{COOH}$ : 0.6%, 1.3%, 2.0%, 2.6%, 3.3% and 4.0% (w/w) of  $\text{Fe}_3\text{O}_4@\text{C-COOH}$  were added to lead-contaminated soil with water content adjusted to 50%. After 10 days of exposure, the chemical state of the soil samples was analysed to determine the effect of  $\text{Fe}_3\text{O}_4@\text{C-COOH}$  AM on Pb speciation.
- (2) Soil pH: To investigate the effect of pH on the efficacy of the  $\text{Fe}_3\text{O}_4@\text{C-COOH}$  nanoparticles,  $\text{HNO}_3$  and NaOH were used to regulate the pH of the tested soils. After aging, the measured pH values were 6.41, 6.92, 7.33, 7.96, 8.52 and 9.87.  $\text{Fe}_3\text{O}_4@\text{C-COOH}$  was added at 3.3% (w/w) following the procedure described for the AA experiment. After 10 days of exposure, the soil Pb chemical state analysis was conducted to determine the effect of soil pH on the speciation distribution of Pb.
- (3) Water content (WC): An AA of 3.3%  $\text{Fe}_3\text{O}_4@\text{C-COOH}$  was added to contaminated soil and the WC was adjusted to 20%, 30%, 40%, 50%, 60% and 70% using distilled water. The pH for all treatments was treated to 7.33 per the procedure described for the soil pH experiment. Following 10 days of exposure, the soil Pb chemical state analysis was conducted to determine the effect of soil WC on the speciation distribution of Pb.
- (4) Electrical conductivity (EC): The effects of  $\text{Fe}_3\text{O}_4@\text{C-COOH}$  on the chemical state of Pb under different EC conditions were studied using an  $\text{Fe}_3\text{O}_4@\text{C-COOH}$  AA of 3.3%, pH of 7.33 and WC at 50%. Treatment for WC was conducted per the procedure described for the soil WC experiment. EC was adjusted to 96.5, 142.6, 175.4, 253.1, 316.2, 358.1 and  $358.1 \mu\text{S}\cdot\text{cm}^{-1}$  using KCl.
- (5) Organic matter (OM): The effects of  $\text{Fe}_3\text{O}_4@\text{C-COOH}$  on the chemical state of Pb under different OM conditions were studied using an  $\text{Fe}_3\text{O}_4@\text{C-COOH}$  AA of 3.3%, pH of 7.33, WC at 50% and EC adjusted to  $142.6 \mu\text{S}\cdot\text{cm}^{-1}$  per the procedure described for the soil EC experiment. Soil OM was adjusted to  $20.13 \text{ g}\cdot\text{kg}^{-1}$ ,  $32.33 \text{ g}\cdot\text{kg}^{-1}$ ,  $45.26 \text{ g}\cdot\text{kg}^{-1}$ ,  $51.72 \text{ g}\cdot\text{kg}^{-1}$ ,  $63.04 \text{ g}\cdot\text{kg}^{-1}$ , and  $79.20 \text{ g}\cdot\text{kg}^{-1}$  using humus (Tianjin Guangfu Fine Chemical Research Institute, Tianjin, CHN).
- (6) Immobilisation stability effect: Following 5, 10, 30, 60, 90 and 180 days of exposure, the chemical

state of Pb was analysed to determine the effect of immobilisation time on Pb state. Parameters of the experiment were as follows:  $\text{Fe}_3\text{O}_4@\text{C-COOH}$  AA (3.3%), pH (7.33), WC (50%) and EC ( $142.6 \mu\text{S}\cdot\text{cm}^{-1}$ ). OM was adjusted to  $63.04 \text{ g}\cdot\text{kg}^{-1}$  per the procedure described for the OM experiment.

The untreated soil was used as the control treatment (CK). Three replicates were prepared for each treatment in each experiment.

### Chemical Analysis

The pH was determined by potentiometry FE20 (METTLER-TOLEDO CO., Ltd, ZURICH, CH) [28]. Briefly summarized here are the following: step 1 (acid soluble state) – the WC was determined by drying method [29]. The EC was determined by the 5:1 extraction method [28]. OM was determined by the potassium dichromate-concentrated sulfuric acid external heating method [30]. Pb contents of water and soil were determined by atomic absorption spectrometer (ZEEnit-700P, Analytik Jena AG, Jena, Germany).

The BCR sequential extraction method with a small modification was used to determine the lead state [31]. Briefly summarized here are the following: step 1 (acid soluble state), accurately taking  $0.5000\text{g}$  sample in a  $40\text{ml}$  centrifuge tube, add  $20 \text{ ml } 0.1\text{mol}\cdot\text{L}^{-1} \text{CH}_3\text{COOH}$ , shake at  $160 \text{ r}\cdot\text{min}^{-1}$  for  $16\text{h}$  at room temperature, centrifuge at  $3000 \text{ r}\cdot\text{min}^{-1}$  for  $20 \text{ min}$ , and take the supernatant to be tested. In the second step (reducible state), the first-step residue was added to  $0.5 \text{ mol}\cdot\text{L}^{-1} \text{NH}_4\text{OH} \cdot \text{HCl}$  and shaken at  $160\pm 5 \text{ r}\cdot\text{min}^{-1}$  for  $16\text{h}$  at room temperature, centrifuged at  $3000 \text{ r}\cdot\text{min}^{-1}$  for  $20\text{min}$ , and the supernatant was sampled. In step 3 (oxidizable state), add  $5 \text{ ml}$  of  $30\% \text{H}_2\text{O}_2$  to the residue of the second step, shake well, and after standing for  $1 \text{ hour}$ , heat the water bath ( $85\pm 2^\circ\text{C}$ ) to nearly dry  $\text{H}_2\text{O}_2$ , cool, and then add  $5 \text{ ml}$  of  $30\% \text{H}_2\text{O}_2$  in a water bath until nearly dry. After cooling, add  $25 \text{ ml}$  of  $1 \text{ mol}\cdot\text{L}^{-1} \text{NH}_4\text{OAc}$  and shake at  $160\pm 5 \text{ r}\cdot\text{min}^{-1}$  for  $16 \text{ h}$  at room temperature. Centrifuge at  $3000 \text{ r}\cdot\text{min}^{-1}$  for  $20 \text{ min}$  and take the supernatant to be tested. The residual soil from step 3 was washed with distilled water, and air-dried soil residues were digested with  $\text{HCl-HNO}_3\text{-HClO}_4$  acids to extract the final residual state. The stability of the acid-soluble and reducible fractions was poor and could be taken up by crops or leached out of the soil; these fractions were bioavailable, while the oxidisable and residual fractions were stable [4, 25]. The effects of AA, soil pH, WC, EC and OM on the distribution of Pb state can be evaluated by observing the conversion rate (CR) of chemical forms of lead from bioavailable to stable (i.e., not biologically available). The CR was calculated as follows:

$$N = \frac{A+B}{F} \quad (1)$$

...where  $A$  is the reducible fraction,  $B$  is the acid soluble fraction,  $F$  is the total Pb, and  $N$  is the CR.

Pb immobilisation efficiency (IE) was calculated as follows:

Where  $C$  is the Pb content of leaching in original soil, and  $D$  is the Pb content of TCLP soil leachate following remediation by immobilisation.

### Statistical Analysis

The data were expressed as the means $\pm$ SD ( $n = 3$ ) and analysed using SPSS 19.0 (SPSS Inc, Chicago, IL, USA). Figures were produced using OriginPro 9.0 (OriginLab, Northampton, Massachusetts, USA). Statistical significance was tested with an independent-sample T Test or one-way analysis of variance (ANOVA) followed by Duncan's multiple range test.

## Results and Discussion

### Characterisation of $\text{Fe}_3\text{O}_4@\text{C-COOH}$

#### *Characterisation and Analysis of $\text{Fe}_3\text{O}_4@\text{C-COOH}$ by SEM and TEM*

SEM and TEM were used to analyse the morphology of  $\text{Fe}_3\text{O}_4@\text{C-COOH}$  (Fig. 2a, 2b). It can clearly be seen from the figures that the internal colour of the material is lighter, delamination is obvious, microspheres are formed, particle size is uniform, dispersion is good,

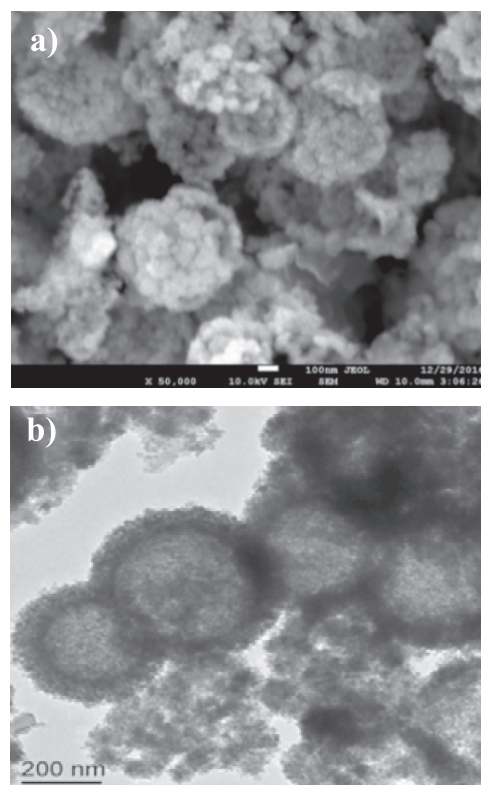


Fig. 2. SEM a) and TEM b) of  $\text{Fe}_3\text{O}_4@\text{C-COOH}$ .

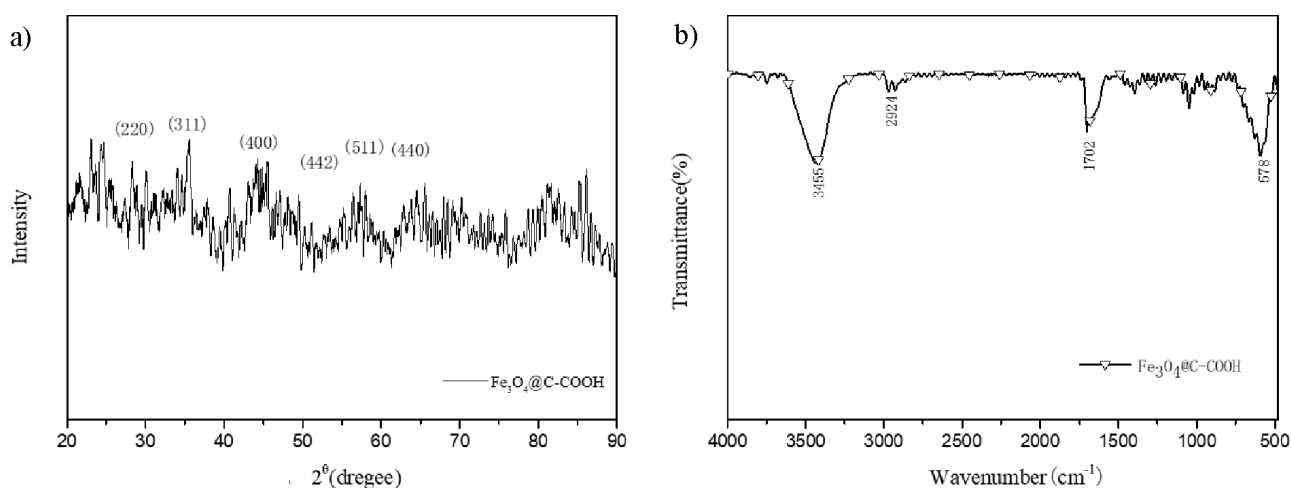


Fig. 3. X-ray diffraction a) and FT-IR b) of  $\text{Fe}_3\text{O}_4@\text{C-COOH}$ .

and the core-shell structure is hollow. The particle size distribution of the hollow microspheres presented in Fig. 2a) indicates a particle size of approximately 400 nm. The structures from the inside to the outside were demonstrated as  $\text{Fe}_3\text{O}_4$  hollow microspheres, carbon shells, and functional groups. The innermost layer, hollow  $\text{Fe}_3\text{O}_4$ , has the properties of non-toxicity and good biocompatibility, allowing for no damage to soil structure and properties, and having no effect on groundwater. The middle layer, carbon shell, can protect  $\text{Fe}_3\text{O}_4$  from oxidation and prevent the microspheres from rejoining, while maintaining excellent stability under extreme conditions of acidity, alkalinity, temperature and pressure [32]. This property allows for application in a wide range of soil pH.

#### *XRD and Infrared Spectrum Characterisation Analysis*

The crystal structure of  $\text{Fe}_3\text{O}_4@\text{C-COOH}$  was characterised with XRD (Fig. 3a). The characteristic  $2\theta$  peaks of aminated  $\text{Fe}_3\text{O}_4@\text{C}$  magnetic nanoparticles were found at  $30.1^\circ$ ,  $35.5^\circ$ ,  $43.2^\circ$ ,  $53.4^\circ$ ,  $57.1^\circ$  and  $62.6^\circ$ . The diffraction fronts correlate with the crystal shapes and corresponding structures of (220), (311), (400), (442), (511), (440), respectively. These results are generally consistent with the standard XRD spectra of  $\text{Fe}_3\text{O}_4$ ; however, the width of the diffraction peaks differs, which is related to the change in particle size. The characteristic XRD peaks of carboxylated  $\text{Fe}_3\text{O}_4@\text{C-COOH}$  are relatively weak, indicating that the presence of functional groups weakens the intensity of the characteristic peaks and indirectly indicates that a substance is attached to the material [33]. Thus,  $\text{Fe}_3\text{O}_4@\text{C-COOH}$  nanoparticles essentially maintain the spinel structure of  $\text{Fe}_3\text{O}_4$ .

The chemical composition and functional groups of  $\text{Fe}_3\text{O}_4@\text{C-COOH}$  were characterised by Fourier transform infrared spectroscopy (FT-IR). In Fig. 3b), the broad peak near  $3455\text{ cm}^{-1}$  is the stretching vibration

absorption peak of -OH, the characteristic absorption peak at  $578\text{ cm}^{-1}$  is  $\text{Fe}_3\text{O}_4$ , and the stretching vibration peak at  $2924\text{ cm}^{-1}$  corresponds to C-H. A strong peak at  $1702\text{ cm}^{-1}$  was identified as the characteristic absorption peak of -COOH, which forms the mercaptopropionic acid of the polymer. Thus it can be seen that -COOH has been successfully attached to the surface of  $\text{Fe}_3\text{O}_4@\text{C}$ . Considering the results shown in both Figs 2a) and 2b), it can be concluded that a layer of functional groups has attached to surface material of the hollow core-shell structure, thus enhancing the specificity of Pb [34].

#### *Determining Magnetic Properties*

The magnetic properties of  $\text{Fe}_3\text{O}_4@\text{C-COOH}$  were tested using VSM (EZ7, MicroSense, USA) at room temperature (300K) to obtain the hysteresis loop (Fig. 4). Evidence of the hysteresis loop demonstrates that the  $\text{Fe}_3\text{O}_4@\text{C-COOH}$  nanoparticles exhibit superparamagnetism. The saturation magnetization of the material was  $60.21\text{ emu}\cdot\text{g}^{-1}$ . The magnetic coercivity

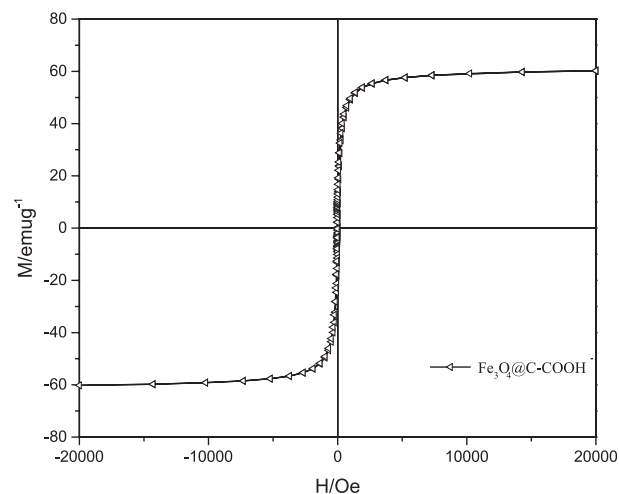


Fig. 4. VSM of  $\text{Fe}_3\text{O}_4@\text{C-COOH}$ .

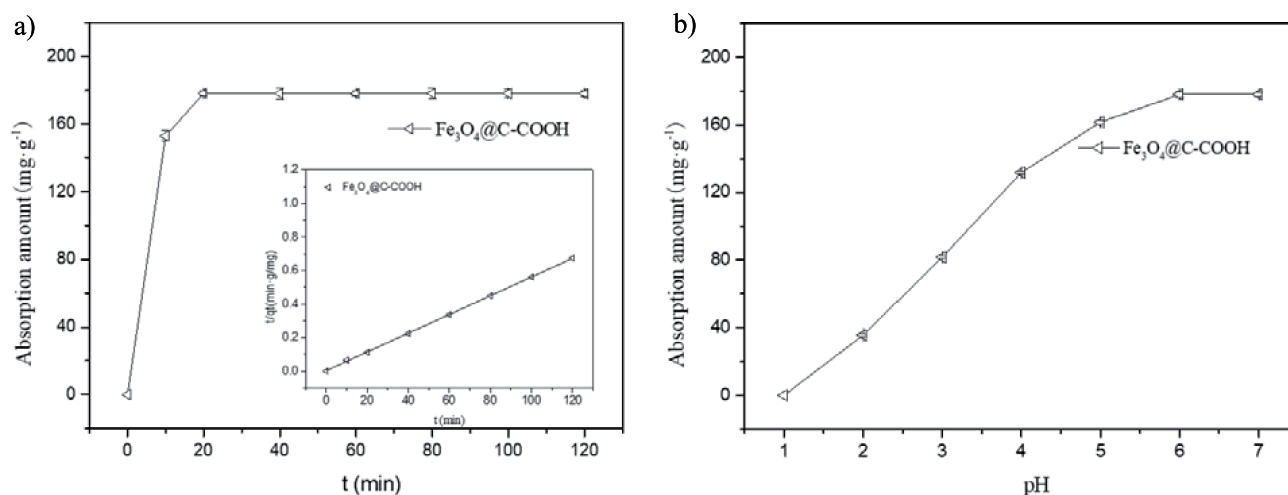


Fig. 5. Effects of adsorption time on adsorption quantities a) and initial concentration on adsorption quantities b).

and remanence of the material tend to zero, leading to superparamagnetism [35-36]. The hysteresis loops illustrate an excellent super-paramagnetic nature, and demonstrate the smooth encapsulation of magnetic nanoparticles without loss of magnetic properties. Magnetism can accelerate the sorption of heavy metal ions in soil by the remediation agent [7, 10], thus promoting transformation to a stable residual state and shortening the remediation time.

#### Adsorption Characteristics of Pb of $\text{Fe}_3\text{O}_4@\text{C-COOH}$ in Water

The adsorption equilibrium of  $\text{Fe}_3\text{O}_4@\text{C-COOH}$  in water was established within 20 minutes with a fast adsorption rate (Fig. 5a). The saturated adsorption capacity of  $\text{Pb}^{2+}$  is  $178.13 \text{ mg}\cdot\text{g}^{-1}$  (Fig. 5b), which suggests that the adsorption of  $\text{Pb}^{2+}$  occurs on the surface of  $\text{Fe}_3\text{O}_4@\text{C-COOH}$ , where there are a large number of binding sites [36]. The experimental data of  $\text{Pb}^{2+}$  adsorption by  $\text{Fe}_3\text{O}_4@\text{C-COOH}$  were analysed using a quasi-second-order kinetic equation as follows:

$$\frac{t}{q_t} = \frac{1}{K_d q_e^2} + \frac{1}{q_e} t$$

...where  $q_t$  is the adsorption capacity of  $\text{Pb}^{2+}$  that is absorbed by adsorbents at time  $t$  (min),  $\text{mg}\cdot\text{g}^{-1}$ ;  $q_e$  is the adsorption capacity of heavy metal ions that are absorbed by adsorbents at adsorption equilibrium,  $\text{mg}\cdot\text{g}^{-1}$ ; and  $K_{ad}$  is the rate constant of quasi-second-order adsorption kinetics,  $\text{g}\cdot(\text{mg}\cdot\text{min})^{-1}$ .

Using the quasi second-order kinetic equation to fit the curve, plots of  $t/q_t$  versus  $t$  exhibit a straight line. The corresponding calculations of  $q_e$ ,  $K_{ad}$  and  $R^2$  are shown in Table 2, which shows that the correlation coefficient  $R^2 \approx 1$  of the quasi second-order kinetic equation indicates that the regression model coincides well with the data points. Therefore, the quasi second-order kinetic equation can be used to describe the adsorption process of adsorbents for  $\text{Pb}^{2+}$ . This further indicates that the rate-limiting step of adsorption is controlled by the chemical adsorption between adsorbent and adsorbate [37], and is not affected by substance transfer in solution [38-39]. In addition, the value of  $q_e$  calculated with the quasi second-order kinetic equation was  $179.21 \text{ mg}\cdot\text{g}^{-1}$ , which is similar to the experimental value of  $178.13 \text{ mg}\cdot\text{g}^{-1}$  (Fig. 5b).

#### Effect of $\text{Fe}_3\text{O}_4@\text{C-COOH}$ AA on Distribution of Pb State

The application of  $\text{Fe}_3\text{O}_4@\text{C-COOH}$  has a significant effect on the fractionation of lead by promoting a change from acid-soluble and reducible to a residual state (Fig. 6a). With increasing amounts of  $\text{Fe}_3\text{O}_4@\text{C-COOH}$ , the CR first increases rapidly and then increases slowly (Fig. 6a). After adding 0.6%, 1.3%, 2.0%, 2.6%, 3.3% and 4.0% (w/w)  $\text{Fe}_3\text{O}_4@\text{C-COOH}$  to lead-contaminated soils, the CR was  $3.76 \pm 0.25\%$ ,  $16.17 \pm 1.34\%$ ,  $15.07 \pm 1.17\%$ ,  $18.02 \pm 2.22\%$ ,  $19.67 \pm 1.68\%$  and  $21.25 \pm 1.34\%$ , respectively. When the amount was more than 3.3%, the conversion effect experienced a lesser change. Therefore, in the lead-contaminated soil the AA of  $\text{Fe}_3\text{O}_4@\text{C-COOH}$  at 3.3% was suitable. At this AA, the acid-soluble Pb is 9.68%,

Table 2. Quasi second-order kinetic equation fitting data.

Category	Equation	$R^2$	$K_{ad}$	$q_e$
$\text{Fe}_3\text{O}_4@\text{C-COOH}$	$y = 0.00558 + 0.00277x$	0.99982	0.0112	179.21

the reducible Pb was 47.38%, the oxidisable Pb was 20.04%, the residual Pb was 23.31%, and the CR of Pb was 19.67±1.68%.

*Effect of Soil pH on Distribution of Pb State*

Soil pH plays a crucial role in the mobility and bioavailability of heavy metals [15]. The pH has a

small effect on the fractionation of lead (Fig. 6b): with increasing pH, the CR gradually increased, and reached a plateau when the pH was greater than 7.33 (Fig. 5a). The CR was 15.86±0.99%, 16.32±1.51%, 20.01±1.54%, 19.26±2.01%, 20.02±1.78% and 19.73±2.54% with a soil pH of 6.41, 6.92, 7.33, 7.96, 8.52 and 9.87, respectively. Within a pH range of 6.41 to 9.87, the CR does not change significantly, indicating that the Fe<sub>3</sub>O<sub>4</sub>@C-COOH has a wide range of application based on resistance to

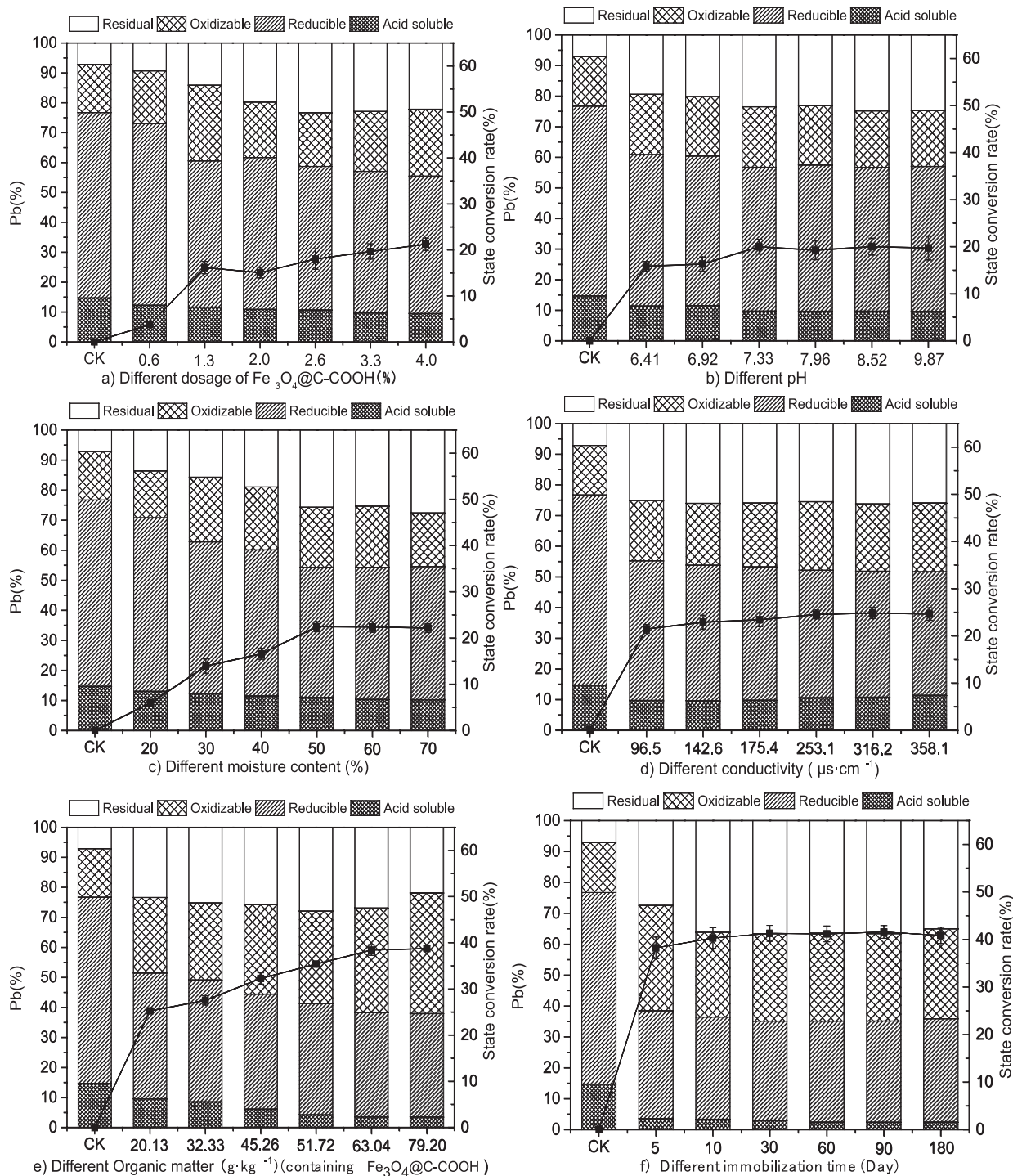


Fig. 6. Effects of Fe<sub>3</sub>O<sub>4</sub>@C-COOH amount a); pH b); water content c); electrical conductivity d); organic matter e); and immobilisation time f) on the distribution of Pb state and conversion rate of Pb state.

strong acids and bases. Thus, the appropriate pH range should be maintained between 6 and 10; in this case, the original soil pH was 7.33 and would not require adjustment. At this pH, the acid-soluble Pb was 9.70%, the reducible Pb was 47.02%, the oxidisable Pb was 19.80%, and the residual Pb was 23.89%.

#### *Effect of Soil WC on Distribution of Pb State*

The bioavailability of heavy metals in soils is affected by multiple factors, including pH, temperature, nutrient concentration and available WC [40]. The solubility and bioavailability of heavy metals in soils are mainly dependent on soil pH and redox potential (Eh), and the Eh can be significantly affected by water content [15]. WC has a significant effect on the fractionation of lead, and promotes the transformation of soil Pb from the reducible to residual state (Fig. 6c). With increasing WC, the CR gradually increases; when the WC is greater than 50%, there is little change in the CR (Fig. 5a). The CR was  $5.94\pm 0.19\%$ ,  $13.95\pm 1.56\%$ ,  $16.61\pm 1.17\%$ ,  $22.46\pm 1.08\%$ ,  $22.41\pm 1.12\%$  and  $22.18\pm 0.95\%$  with a soil WC of 20%, 30%, 40%, 50%, 60% and 70%, respectively. These results indicate that when the WC is greater than 50%, WC is no longer a limiting factor affecting Pb exposure to  $\text{Fe}_3\text{O}_4\text{-C-COOH}$  in soil.

#### *Effect of Soil EC on Distribution of Pb State*

Soil EC has an insignificant effect on distribution of Pb fractions when promoting a change in soil Pb from the reducible to residual state (Fig. 6d). With increasing EC, the CR exhibits little change. The CR was  $21.47\pm 0.94\%$ ,  $22.90\pm 1.48\%$ ,  $23.43\pm 1.46\%$ ,  $24.55\pm 0.93\%$ ,  $24.86\pm 1.16\%$  and  $24.65\pm 1.32\%$  when the soil EC was adjusted to 96.5, 142.6, 175.4, 253.1, 316.2, 358.1 and  $358.1 \mu\text{S}\cdot\text{cm}^{-1}$ , respectively, which indicates that  $\text{Fe}_3\text{O}_4\text{-C-COOH}$  nanoparticles have a wide application range of salinity.

#### *Effect of Soil OM on Distribution of Pb sState*

Soil OM has a significant effect on the fractionation of lead, and promotes the change in soil Pb from acid-soluble and reducible to the residual state (Fig. 6e). With increasing OM, the CR increased; when OM is greater

than  $63.04 \text{ g}\cdot\text{kg}^{-1}$ , there is little change in CR (Fig. 7). The CR was  $25.26\pm 0.21\%$ ,  $27.54\pm 1.01\%$ ,  $32.29\pm 1.22\%$ ,  $35.39\pm 0.61\%$ ,  $38.43\pm 1.16\%$  and  $38.75\pm 0.59\%$  when the soil OM was adjusted to  $20.13 \text{ g}\cdot\text{kg}^{-1}$ ,  $32.33 \text{ g}\cdot\text{kg}^{-1}$ ,  $45.26 \text{ g}\cdot\text{kg}^{-1}$ ,  $51.72 \text{ g}\cdot\text{kg}^{-1}$ ,  $63.04 \text{ g}\cdot\text{kg}^{-1}$  and  $79.20 \text{ g}\cdot\text{kg}^{-1}$ , respectively. These results may be due to the increase of soil OM promoting an increase in cation exchange capacity, which improves the fixation of heavy metals, thus limiting the available state of heavy metals [33, 41-42]. OM and  $\text{Fe}_3\text{O}_4\text{-C-COOH}$  have a synergistic effect of improving morphological CR. In consideration of both the CR and cost, the optimal content of OM was found to be  $63.04 \text{ g}\cdot\text{kg}^{-1}$ .

#### *Stability of Pb State Conversion Effect*

Immobilisation time has a significant effect on engineering construction and remediation expenses, and the stability of Pb state CR directly affects the effectiveness of remediation [15, 25]. Fig. 6f) shows that immobilisation time has no significant effect on the fractionation of lead. The CR was  $38.24\pm 2.26\%$ ,  $40.29\pm 2.18\%$ ,  $41.29\pm 1.68\%$ ,  $41.18\pm 1.66\%$ ,  $41.58\pm 1.35\%$  and  $40.85\pm 1.71\%$  when the exposure time was 5, 10, 30, 60, 90 and 180 days, respectively. This indicates that  $\text{Fe}_3\text{O}_4\text{-C-COOH}$  requires a relatively short residence time to achieve immobilisation of Pb in contaminated soils.

#### *$\text{Fe}_3\text{O}_4\text{-C-COOH}$ IE by TCLP Test Method*

In summary, it can be seen from results of the six immobilisation remediation experiments that the suitable conditions for immobilisation by  $\text{Fe}_3\text{O}_4\text{-C-COOH}$  in lead-contaminated soil are: AA of 3.3%, pH of 7.33, WC of 50%, conductivity of  $142.6 \mu\text{S}\cdot\text{cm}^{-1}$ , OM of  $63.04 \text{ g}\cdot\text{kg}^{-1}$ , and an exposure time of no less than 10 days. However, Pb state could be transferred reciprocally and the transformation impacts the toxicity of heavy metal ions in soil [15, 43-44]. Therefore, a leaching toxicity test (TCLP) is an appropriate method to evaluate the stabilization treatment of heavy metal-contaminated soil [8]. Following remediation by immobilisation under suitable conditions, the standard TCLP test method (USEPA, 1994) was applied to measure plant phytoavailability, bioaccessibility and leaching toxicity of Pb in lead-contaminated soil [45]. The soil TCLP-Pb content before and after remediation were  $24.16\pm 1.03$  and  $3.86\pm 0.35 \text{ mg}\cdot\text{kg}^{-1}$ , respectively (Table 3), and the

Table 3. Changes of soil pH, EC and leaching concentration of Pb before and after remediation.

Soil	pH	EC ( $\mu\text{S}\cdot\text{cm}^{-1}$ )	TCLP-Pb ( $\text{mg}\cdot\text{kg}^{-1}$ )	China standards of TCLP-Pb* ( $\text{mg}\cdot\text{kg}^{-1}$ )	Immobilisation efficiency (%)
Original	$7.33\pm 0.20$ a	$142.60\pm 1.57$ b	$24.16\pm 1.03$ a	5	84.23
After Remediation	$7.31\pm 0.08$ a	$221.37\pm 2.23$ a	$3.86\pm 0.35$ b		

\*Notes: The standard limit refers to GB5085.3-2007. The same letter (a, b) within the same column is not significantly different at  $P<0.05$ .

soil TCLP-Pb content of original soil was significantly lower than that of the remediated soil ( $p < 0.05$ ). The IE reached 84.23% and the soil TCLP-Pb content following remediation was lower than that required by the national standards of China ( $5 \text{ mg}\cdot\text{kg}^{-1}$ ). At the same time, there was no significant difference in soil pH before and after remediation. Although the EC increased from  $142.60 \mu\text{s}\cdot\text{cm}^{-1}$  to  $247.46 \mu\text{s}\cdot\text{cm}^{-1}$ , the remediated soil can still be classified as a non-saline soil and would not affect crop growth. Results of the TCLP test indicate that the goal of remediation by  $\text{Fe}_3\text{O}_4@\text{C-COOH}$  immobilisation was achieved.

### Conclusions

The novel remediation agent  $\text{Fe}_3\text{O}_4@\text{C-COOH}$  was proven to possess a high adsorption capacity with a short equilibrium time, and a wide range of pH and salinity could suit application.  $\text{Fe}_3\text{O}_4@\text{C-COOH}$  nanoparticles promote the transformation of Pb from a reducible to residual state in Pb-contaminated soil. The combination of  $\text{Fe}_3\text{O}_4@\text{C-COOH}$  and OM improved the decrease in soil of the acid-soluble and reducible fractions of Pb. When the WC was more than 50%, water no longer affected Pb immobilisation in soil. In addition, only a short residence time (less than 10 days) was needed for Pb immobilisation to occur with the desired effect of long-term stability. Under suitable conditions, IE can reach 84.23%, which achieves the goal of remediation in Pb-contaminated soil. This study proposes a method for Pb immobilisation in contaminated soil and opens up new avenues for the preparation and application of magnetic materials in soil remediation.

### Acknowledgements

This research was financially supported by the National Natural Science Foundation of China (No. 41501527), and the Zhengzhou University of Light Industry (grant No. 2013BSJJ022).

### Conflict of Interest

The authors declare no conflict of interest.

### References

- ZHANG T., XU W.X., LIN X.N., YAN H.L., MA M., HE Z.Y. Assessment of heavy metals pollution of soybean grains in North Anhui of China. *Science of the Total Environment*, **646**, 914, **2019**.
- DING K.B., WU Q., HANG W., YANG W.J., SÉRÉ G., WANG S.Z., ECHEVARRIA G., TANG Y.T., TAO J., MOREL J.L. Ecosystem services provided by heavy metal-contaminated soils in China. *Journal of Soils & Sediments*, **18** (2), 380, **2018**.
- AHMAD H., CAI C., LIU C. Separation and preconcentration of Pb(II) and Cd(II) from aqueous samples using hyperbranched polyethyleneimine-functionalized graphene oxide-immobilized polystyrene spherical adsorbents. *Microchemical Journal*, **145**, 833, **2019**.
- LI J.N., HASHIMOTO Y., RIYA S., TERADA A., HOU H., SHIBAGAKI Y., HOSOMI M. Removal and immobilization of heavy metals in contaminated soils by chlorination and thermal treatment on an industrial-scale. *Chemical Engineering Journal*, **359**, 385, **2019**.
- LI X.X., WANG X.L., CHEN Y.D., YANG X.Y., CUI Z.J. Optimization of combined phytoremediation for heavy metal contaminated mine tailings by a field-scale orthogonal experiment. *Ecotoxicology and Environmental Safety*, **168**, 1, **2019**.
- DINAKE P., KELEBEMANG R., SEHUBE N. A Comprehensive Approach to State of Lead and Its Contamination of Firing Range Soils: A Review. *Soil & Sediment Contamination*, **28** (4), 431, **2019**.
- LIANG X.F., QIN X., HUANG Q.Q., HUANG R., YIN X.L., WANG L., SUN Y.B., XU Y.M. Mercapto functionalized sepiolite: a novel and efficient immobilization agent for cadmium polluted soil. *Rsc Advances*, **7** (63), 39955, **2017**.
- WANG M., CHEN S.B., HAN Y., CHEN L., WANG D. Responses of soil aggregates and bacterial communities to soil-Pb immobilization induced by biofertilizer. *Chemosphere*, **220**, 828, **2019**.
- TENG Z.D., SHAO W., ZHANG K.Y., HUO Y.Q., LI M. Characterization of phosphate solubilizing bacteria isolated from heavy metal contaminated soils and their potential for lead immobilization. *Journal of Environmental Management*, **231**, 189, **2019**.
- BI J.T., HUANG X., WANG J.K., WANG T., WU H., YANG J.Y., LU H.J., HAO H.X. Oil-phase cyclic magnetic adsorption to synthesize  $\text{Fe}_3\text{O}_4@\text{C}@\text{TiO}_2$ -nanotube composites for simultaneous removal of Pb(II) and Rhodamine B. *Chemical Engineering Journal*, **366**, 50, **2019**.
- MEHMOOD S., IMTIAZ M., BASHIR S., RIZWAN M., IRSHAD S., YUVARAJA G., IKRAM M., AZIZ O., DITTA A., REHMAN S.U., et al. Leaching Behavior of Pb and Cd and Transformation of Their Speciation in Co-Contaminated Soil Receiving Different Passivators. *Environmental Engineering Science* 10.1089/ees.2018.0503, **2019**.
- XIE T., LI Y., DONG H., LIU Y., WANG M., WANG G. Effects and mechanisms on the reduction of lead accumulation in rice grains through lime amendment. *Ecotoxicology and Environmental Safety*, **173**, 266, **2019**.
- HUANG G.Y., GAO R.L., YOU J.W., ZHU J., FU Q.L., HU H.Q. Oxalic acid activated phosphate rock and bone meal to immobilize Cu and Pb in mine soils. *Ecotoxicology and environmental safety*, **174**, 401, **2019**.
- VRINCEANU N.O., MOTELICA D.M., DUMITRU M., CALCIU I., TANASE V., PREDA M. Assessment of using bentonite, dolomite, natural zeolite and manure for the immobilization of heavy metals in a contaminated soil: The Copsa Mica case study (Romania). *Catena*, **176**, 336, **2019**.
- XU Y., LIANG X.F., XU Y.M., QIN X., HUANG Q.Q., WANG L., SUN Y.B. Remediation of Heavy Metal-Polluted Agricultural Soils Using Clay Minerals: A Review. *Pedosphere*, **27** (2), 193, **2017**.

16. BYOUNG CHAN K., JINWOO L., WOYONG U., JAEYUN K., JIN J., HYUNG L.J., JA HUN K., JAE HYUN K., LEE C., LEE H. Magnetic mesoporous materials for removal of environmental wastes. *Journal of Hazardous Materials*, **192** (3), 1140, **2011**.
17. FIGUEIRA P., LOPES C.B., DANIEL-DA-SILVA A.L., PEREIRA E., DUARTE A.C., TRINDADE T. Removal of mercury (II) by dithiocarbamate surface functionalized magnetite particles: application to synthetic and natural spiked waters. *Water Research*, **45** (17), 5773, **2011**.
18. YANG J.B., YU M.Q., QIU T. Adsorption thermodynamics and kinetics of Cr(VI) on KIP210 resin. *Journal of Industrial & Engineering Chemistry*, **20** (2), 480, **2014**.
19. FAN H.L., ZHOU S.F., JIAO W.Z., QI G.S., LIU Y.Z. Removal of heavy metal ions by magnetic chitosan nanoparticles prepared continuously via high-gravity reactive precipitation method. *Carbohydrate Polymers*, **174**, 1192, **2017**.
20. MA C., LI C., HE N., WANG F., MA N., ZHANG L., LU Z., ALI Z., XI Z., LI X. Preparation and characterization of monodisperse core-shell Fe<sub>3</sub>O<sub>4</sub>@SiO<sub>2</sub> microspheres and its application for magnetic separation of nucleic acids from *E. coli* BL21. *Journal of Biomedical Nanotechnology*, **8** (6), 1000, **2012**.
21. SAHRAEI R., POUR Z.S., GHAEMY M. Novel magnetic bio-sorbent hydrogel beads based on modified gum tragacanth/graphene oxide: Removal of heavy metals and dyes from water. *Journal of Cleaner Production*, **142** (4), 2973, **2017**.
22. KIM B.C., LEE J., UM W., KIM J., JIN J., JIN H.L., KWAK J.H., KIM J.H., LEE C.H., LEE H.S. Magnetic mesoporous materials for removal of environmental wastes. *Journal of Hazardous Materials*, **192** (3), 1140, **2011**.
23. PÅL G., EILIV S. Influence of pH and TOC concentration on Cu, Zn, Cd, and Al speciation in rivers. *Water Research*, **37** (2), 307, **2003**.
24. CHENG Z.L., TAN A.L.K., TAO Y., SHAN D., TING K.E., YIN X.J. Synthesis and Characterization of Iron Oxide Nanoparticles and Applications in the Removal of Heavy Metals from Industrial Wastewater. *International Journal of Photoenergy* 10.1155/2012/608298, **2012**.
25. ZONG Y.T., XIAO Q., LU S.G. Chemical fraction, leachability, and bioaccessibility of heavy metals in contaminated soils, Northeast China. *Environmental Science and Pollution Research*, **23** (23), 24107, **2016**.
26. LIU L.Y., WANG X.F., ZHANG C.X., CHENG B. Preparation of SiO<sub>2</sub> microspheres used in photonic crystals via improving stober method. *Materials Review*, **22** (12), 113, **2008** [In Chinese].
27. CHENG K., SUN Z.Y., ZHOU Y.M., ZHONG H., KONG X.K., XIA P., GUO Z., CHEN Q.W. Preparation and biological characterization of hollow magnetic Fe<sub>3</sub>O<sub>4</sub>@C nanoparticles as drug carriers with high drug loading capability, pH-control drug release and MRI properties. *Biomaterials Science*, **1** (9), 965, **2013**.
28. JAYASINGHE G.Y., TOKASHIKI KITOU. Evaluation of Coal Fly Ash-Based Synthetic Aggregates as a Soil Ameliorant for the Low Productive Acidic Red Soil. *Water Air & Soil Pollution*, **204** (1-4), 29, **2009**.
29. LIU X., GUO K., HUANG L., JI Z., JIANG H., LI H., ZHANG J. Responses of absolute and specific enzyme activity to consecutive application of composted sewage sludge in a Fluventic Ustochrept. *Plos One*, **12** (5), e0177796, **2017**.
30. SHUAI Y.F., LI X.Y., BIAN J. Determination and analysis of soil organic matter content in greenhouses around Lhasa City. *Agricultural Science & Technology*, **18** (5), 830, **2017**.
31. RIZWAN M.S., IMTIAZ M., HUANG G., CHHAJRO M.A., LIU Y., FU Q., ZHU J., ASHRAF M., ZAFAR M., BASHIR S. Immobilization of Pb and Cu in polluted soil by superphosphate, multi-walled carbon nanotube, rice straw and its derived biochar. *Environmental Science & Pollution Research*, **23** (15), 1, **2016**.
32. ZHAO X.L., SHI Y.L., WANG T., CAI Y.Q., JIANG G.B. Preparation of silica-magnetite nanoparticle mixed hemimicelle sorbents for extraction of several typical phenolic compounds from environmental water samples. *Journal of Chromatography A*, **1188** (2), 140, **2008**.
33. YANG T.Z., SHEN C.M., LI Z., ZHANG H.R., XIAO C.W., CHEN S.T., XU Z.C., SHI D.X., LI J.Q., GAO H.J. Highly ordered self-assembly with large area of Fe<sub>3</sub>O<sub>4</sub> nanoparticles and the magnetic properties. *Journal of Physical Chemistry B*, **109** (49), 23233, **2005**.
34. GUO S., DAN Z., DUAN N., CHEN G., GAO W., ZHAO W. Zn(II), Pb(II), and Cd(II) adsorption from aqueous solution by magnetic silica gel: preparation, characterization, and adsorption. *Environmental Science and Pollution Research*, **25** (31), 30938, **2018**.
35. SU P.F., CHEN G., ZHAO J. Convenient Preparation and Characterization of Surface Carboxyl-functioned Fe<sub>3</sub>O<sub>4</sub> Magnetic Nanoparticles. *Chemical Journal Of Chinese Universities*, **32** (7), 1472, **2011** [In Chinese].
36. JIAO L., QI P.S., LIU Y.Z., WANG B., SHAN L.L. Fe<sub>3</sub>O<sub>4</sub> Nanoparticles Embedded Sodium Alginate/PVP/ Calcium Gel Composite for Removal of Cd<sup>2+</sup>. *Journal of Nanomaterials* 10.1155/2015/940985, **2015**.
37. LIN Y.F., CHEN H.W., CHIEN P.S., CHIOU C.S., LIU C.C. Application of bifunctional magnetic adsorbent to adsorb metal cations and anionic dyes in aqueous solution. *Journal of Hazardous Materials*, **185** (2), 1124, **2011**.
38. ROONASI P., HOLMGREN A. An ATR-FTIR study of sulphate sorption on magnetite; rate of adsorption, surface speciation, and effect of calcium ions. *Journal of Colloid and Interface Science*, **333** (1), 27, **2009**.
39. JOHNSON S.B., FRANKS G.V., SCALES P.J., BOGER D.V., HEALY T.W. Surface chemistry-rheology relationships in concentrated mineral suspensions. *International Journal of Mineral Processing*, **58** (1), 267, **2000**.
40. ALLOWAY B.J. Heavy Metals and Metalloids as Micronutrients for Plants and Animals Heavy Metals in Soils, **22**, 195, **2013**.
41. WALKER D.J., RAFAEL C., M PILAR B. Contrasting effects of manure and compost on soil pH, heavy metal availability and growth of *Chenopodium album* L. in a soil contaminated by pyritic mine waste. *Chemosphere*, **57** (3), 215, **2004**.
42. SHAWABKEH R.A. Solidification and stabilization of cadmium ions in sand-cement-clay mixture. *Journal of Hazardous Materials*, **125** (1), 237, **2005**.
43. LIU W., WANG S.T., PENG L., SUN H.W., HOU J., ZUO Q.Q., RONG H. Response of CaCl<sub>2</sub>-extractable heavy metals, polychlorinated biphenyls, and microbial communities to biochar amendment in naturally contaminated soils. *Journal of Soils & Sediments*, **16** (2), 476, **2016**.

- 
44. ZHANG L.W., SHANG Z.B., GUO K.X., CHANG Z.X., LIU H.L., LI D.L. Speciation analysis and speciation transformation of heavy metal ions in passivation process with thiol-functionalized nano-silica. *Chemical Engineering Journal*, **369**, 979, **2019**.
45. FAYIGA A.O., SAHA U.K. Effect of Phosphate Treatment on Pb Leachability in Contaminated Shooting Range Soils. *Journal of Soil Contamination*, **26** (1), 115, **2017**.

